Japan Society of Histochemistry and Cytochemistry
Established 1959

Acta Histochem. Cytochem. 57 (2): 57–66, 2024
doi: 10.1267/ahc.24-00010

Regular Article

Pathophysiological Implications of Protein Lactylation in Pancreatic Epithelial Tumors

Tomoki Takata[1,3,*], Akihiro Nakamura[2,*], Hiroaki Yasuda[3], Hayato Miyake[3], Yoshio Sogame[3], Yuki Sawai[3], Michiyo Hayakawa[1], Kentaro Mochizuki[1], Ryuta Nakao[1], Takehiro Ogata[1], Hisashi Ikoma[4], Eiichi Konishi[5], Yoshinori Harada[1], Eigo Otsuji[4], Yoshito Itoh[3] and Hideo Tanaka[1]

[1]Department of Pathology and Cell Regulation, Graduate School of Medical Science, Kyoto Prefectural University of Medicine, Kyoto, Japan , [2]Central Research Facility, Graduate School of Medical Science, Kyoto Prefectural University of Medicine, Kyoto, Japan , [3]Department of Molecular Gastroenterology and Hepatology, Graduate School of Medical Science, Kyoto Prefectural University of Medicine, Kyoto, Japan , [4]Division of Digestive Surgery, Department of Surgery, Graduate School of Medical Science, Kyoto Prefectural University of Medicine, Kyoto, Japan and [5]Department of Surgical Pathology, Graduate School of Medical Science, Kyoto Prefectural University of Medicine, Kyoto, Japan

Received January 19, 2024; accepted February 2, 2024; published online April 4, 2024

Protein lactylation is a post-translational modification associated with glycolysis. Although recent evidence indicates that protein lactylation is involved in epigenetic gene regulation, its pathophysiological significance remains unclear, particularly in neoplasms. Herein, we investigated the potential involvement of protein lactylation in the molecular mechanisms underlying benign and malignant pancreatic epithelial tumors, as well as its role in the response of pancreatic cancer (PC) cells to gemcitabine. Increased lactylation was observed in the nuclei of intraductal papillary mucinous adenoma, non-invasive intraductal papillary mucinous carcinoma, and invasive carcinoma, in parallel to the upregulation of hypoxia-inducible factor-1α. This observation indicated that a hypoxia-associated increase in nuclear protein lactylation could be a biochemical hallmark in pancreatic epithelial tumors. The standard PC chemotherapy drug gemcitabine suppressed histone lactylation *in vitro*, suggesting that histone lactylation might be relevant to its mechanism of action. Taken together, our findings suggest that protein lactylation may be involved in the development of pancreatic epithelial tumors and could represent a potential therapeutic target for PC.

Key words: lactylation, pancreatic epithelial tumor, gemcitabine, acetylation

I. Introduction

Pancreatic cancer (PC) accounted for 3.3% of all cancer cases in 2023, and its incidence is gradually increasing at a rate of 1% per year [1, 4]. PC has an especially poor prognosis among all human cancers, with a 5-year survival rate of approximately 12.5% [4]. Further, less than 20% of the patients with PC can undergo surgery [20]. Although some chemotherapeutic regimens have been established, their efficacy in extending survival remains limited owing to the development of drug resistance (e.g., gemcitabine (GEM)) and/or serious side effects (e.g., the FOLFIRINOX

* These authors contributed equally to this work.

Correspondence to: Akihiro Nakamura, Ph. D., Central Research Facility, Graduate School of Medical Science, Kyoto Prefectural University of Medicine, 465 Kajii-Cho Kamigyo-Ku, Kyoto 602–8566, Japan.
E-mail: nakam993@koto.kpu-m.ac.jp
Yoshinori Harada, M. D., Ph. D., Department of Pathology and Cell Regulation, Graduate School of Medical Science, Kyoto Prefectural University of Medicine, 465 Kajii-Cho Kamigyo-Ku, Kyoto 602–8566, Japan. E-mail: yoharada@koto.kpu-m.ac.jp

regimen) [6, 17]. The same holds true for radiation therapy, likely due to low oxygen tension within the tumor microenvironment [21].

Recent studies have suggested the involvement of altered cellular metabolism in the molecular pathogenesis of PC. Indeed, PC grows despite the harsh hypoxic microenvironment formed due to hypovascularity and dense desmoplasia-associated decreases in local blood flow [22]. Such a severely hypoxic microenvironment triggers a switch to glycolysis-dependent energy metabolism through the stabilization of hypoxia-inducible factor 1α (HIF-1α) [31].

In addition to hypoxia-induced metabolic remodeling, some PC-associated gene mutations also promote glycolysis, giving rise to so-called aerobic glycolysis [24, 28]. For example, KRAS, which is mutated in 90% of the PC cases, suppresses the entry of pyruvate into the tricarboxylic acid cycle by activating pyruvate dehydrogenase kinase to upregulate glycolysis, regardless of local oxygen tension [8]. Consequently, glycolysis-dominant energy metabolism sustains PC growth by ramping up ATP generation and adapting oxidative stress.

In light of this glycolysis-dominant metabolism, studies have shed light on the possible pathophysiological significance of lactate, an end-product of glycolysis, in cancer [9]. A recent study revealed that lactate can covalently bind to lysine residues on cellular proteins in a process known as protein lactylation [29]. Although the biological significance of this posttranslational protein modification (PTM) is still incomplete, lactylation has been shown to preferentially target histones and thus epigenetically regulate gene expression [7, 25, 29]. Yang *et al.* reported that protein lactylation levels in tumor tissues are associated with poor prognosis in human gastric cancer [26], implying that lactylation plays a pivotal role in cancer etiology.

At present, little is known regarding the pathophysiological significance of protein lactylation in pancreatic epithelial tumors. As enhanced glycolysis is a hallmark of PC, the involvement of lactylation in PC etiology is of considerable relevance. Herein, based on the analysis of surgical specimens and cultured PC cells, we explored the potential involvement of protein lactylation in the molecular mechanisms of benign and malignant pancreatic epithelial tumors. Additionally, we examined the effect of GEM, a representative chemotherapy for PC, on histone lactylation.

II. Materials and Methods

Clinical study

Patients who underwent surgical removal of pancreatic epithelial tumors at the Kyoto Prefectural University Hospital between January 2010 and April 2012 were included in the study. In particular, patients who had not received chemotherapy or radiation therapy before surgery were evaluated. Two pathologists performed the histological diagnosis of tumors, classifying them as per the WHO classification of tumors of the pancreas, 5th edition, and the 2017 TNM classification of malignant tumors, 8th edition [3]. Representative paraffin-embedded specimens from each patient were selected such that tumor and non-tumor areas were contained within the same section. Samples were then cut into two or three consecutive 4-μm-thick slices. Sections were subjected to hematoxylin and eosin (H&E) and immunostaining using standard protocols. After microwave antigen retrieval, immunohistochemical staining was performed using antibodies against lactyllysine (Kla) (1:10000, #PTM-1401, anti-L-lactyllysine rabbit pAb, PTM Biolabs Inc., Chicago, Illinois, USA) and hypoxia-inducible factor 1α (HIF-1α) (1:300, #20960-1-AP, Proteintech Group, Inc., Rosemont, Illinois, USA). Primary antibodies were visualized using Histofine Simple Stain MAX PO (Nichirei, Tokyo, Japan) and 3, 3-diaminobenzidine tetrahydrochloride (DAB) (Sigma-Aldrich, Missouri, USA). Immuno-control experiments were performed using an identical protocol, except for omission of the primary antibodies (Supplementary Fig. S2). Stained sections were photographed with a NanoZoomer S360 Digital Slide Scanner (Hamamatsu Photonics, Hamamatsu, Japan). For the semi-quantitative analysis of signal intensity (SI) in IHC images, regions of interest (ROIs) were set over tumor sites and adjacent non-tumorous cuboid cells of the interlobular ducts (duct cells)/acinar cells. As inter-specimen differences in DAB SI can cause inconsistent results, we semi-quantified the sample-dependent variation, adopting the ratio calculation of DAB SI in a sample. For the evaluation of lactyllysine SI in non-tumor tissues (Fig. 1D), ratio values were obtained by dividing SI of duct and acinar cell nuclei by that of the cytoplasm. For the semi-quantitative SI analysis of lactyllysine and HIF-1α expression in tumor tissues (Fig. 2), ratios were calculated by dividing the SI of tumor nuclei by that of adjacent non-tumorous duct cell nuclei. The ratio values of the ROIs were calculated using ImageJ (National Institutes of Health, Bethesda, Maryland, USA). Fifty tumor/non-tumor cells in ROIs were arbitrarily selected to calculate SI ratios of lactyllysine and HIF-1α. This study was conducted in accordance with the ethical guidelines of the Declaration of Helsinki and approved by the Ethics Committee of the Kyoto Prefectural University of Medicine (ERB-C-1941-1).

Cell culture

A pancreatic cancer cell line, PANC-1, was purchased from RIKEN BRC CELL BANK (Ibaraki, Japan) and maintained in Dulbecco's modified Eagle's medium (DMEM) (1 g/L glucose) (Nacalai Tesque, Inc., Kyoto, Japan) containing 10% fetal calf serum (FCS) and antibiotics. For the hypoxia study, cells were allowed to grow under the humidified normoxic (18.6% O_2, 5% CO_2) or hypoxic conditions (0.7% O_2, 5% CO_2) for 48 hr. The latter was accomplished using Desk Top Hypoxia Incubator

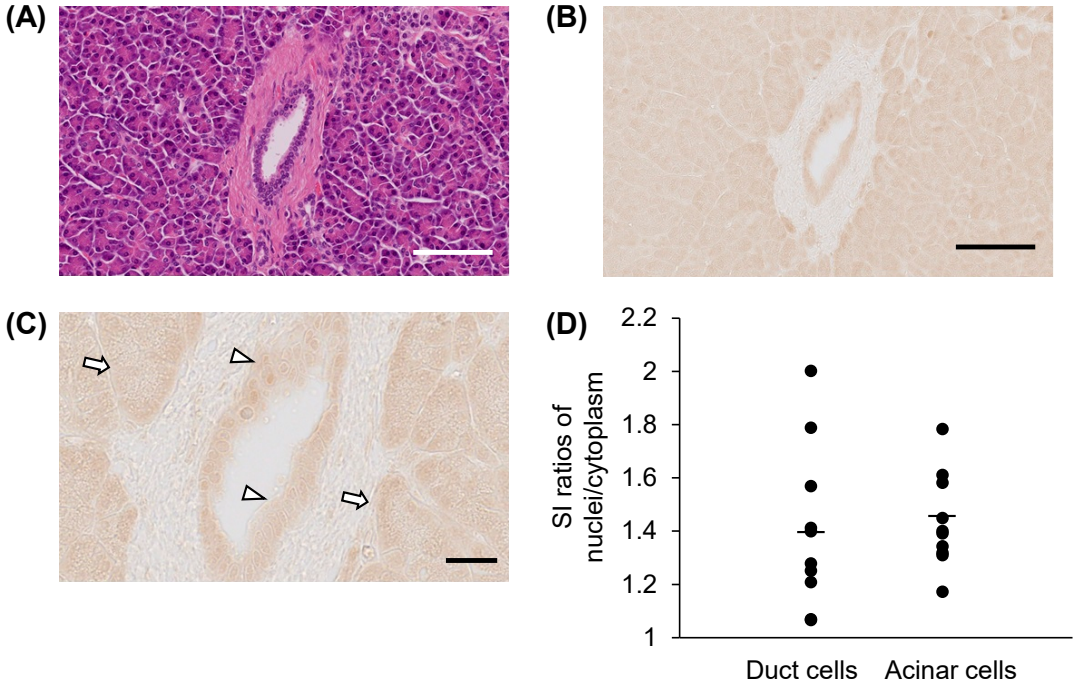

Fig. 1. Immunohistochemical analysis of protein lactylation in non-tumor interlobular ducts and acinar cells in the human pancreas. Representative images of a hematoxylin and eosin-stained section (**A**) and lactyllysine (Kla) immunohistochemistry (IHC) (low-power view: **B**, medium-power view: **C**) are shown. The arrows and arrowheads indicate acinar cells and interlobular duct cells, respectively. Bars = 100 μm (**A**, **B**) and 25 μm (**C**). **D**) Ratios between signal intensities (SIs) in the nuclei and cytoplasm of duct cells (a total of 10 cases, 50 cells per a case) and acinar cells (a total of 10 cases, 50 cells per a case) in Kla IHC images. The short horizontal lines show average values.

SH-140A (BLAST, Kawasaki, Japan). In some experiments, cells were treated with GEM (TCI Chemical, Tokyo, Japan) or sodium butyrate (SB) (TCI Chemicals, Tokyo) under the conditions indicated in figure legends. Living cells were counted using trypan blue dye.

Biochemical study

The cells were washed with phosphate-buffered saline (–) and lysed with 0.0625 M Tris-HCl buffer (pH 6.8) containing 2% sodium dodecyl sulfate (SDS) and 10% glycerol. DNA was sheared with MYJECTOR 29G × 1/2 (TERUMO, Tokyo, Japan). Protein concentration was determined using a BCA protein assay. After reduction and heating, cellular proteins were subjected to immunoblotting with an antibody against lactyllysine (#PTM-1401, PTM Biolabs Inc., Chicago, Illinois). For subcellular fractionation, the cells were disrupted in 20 mM HEPES buffer (pH 7.4) containing 0.25 M sucrose, 1.5 mM $MgCl_2$, 2 mM KCl, 0.5% Triton X100, and proteinase inhibitor cocktail (Nacalai Tesque, Inc., Kyoto). The lysate was centrifuged at 2000 × *g* and 4°C for 10 min. The supernatant was designated as the cytoplasmic fraction. Insoluble materials were resuspended in the same buffer and centrifuged under identical conditions. The resulting pellets were designated as nuclear fractions. Successful subcellular fractionation was confirmed via immunoblotting with antibodies against β-tubulin (cytoplasm) (#014-25041, Fuji film/Wako, Tokyo, Japan) and histone H3 (nucleus) (#819411, BioLegend, San Diego, California, USA).

Histone extraction

Histones were extracted from PANC-1 cells via an acid extraction method [18] with slight modifications. In brief, cells were disrupted with 20 mM HEPES buffer (pH 7.4) containing 0.25 M sucrose, 1.5 mM $MgCl_2$, 2 mM KCl, 0.5% Triton X100, and proteinase inhibitor cocktail, followed by centrifugation at 2000 × *g* and 4°C for 10 min. The pellet was resuspended in the same buffer and centrifuged under the same conditions. The resulting pellets were suspended in 0.2 M sulfuric acid and left on ice for 2 hr with occasional agitation. The suspension was then spun down at 12,000 × *g* and 4°C for 10 min. The supernatant was mixed with a 10-fold volume of ice-cold ethanol and left at −20°C overnight. After centrifugation at 12,000 × *g* and 4°C for 10 min, pellets (histone-enriched fraction) were dissolved in 0.0625 M Tris-HCl buffer (pH 6.8) containing 2% SDS and 10% glycerol, reduced and followed by immunoblotting with an antibody to acetyllysine (#sc-32268, Santa Cruz Biotech, Dallas, Texas, USA), lactyllysine (#PTM-1401, PTM Biolabs Inc., Chicago, Illinois), or histone H3 (#819411, BioLegend, San Diego, California).

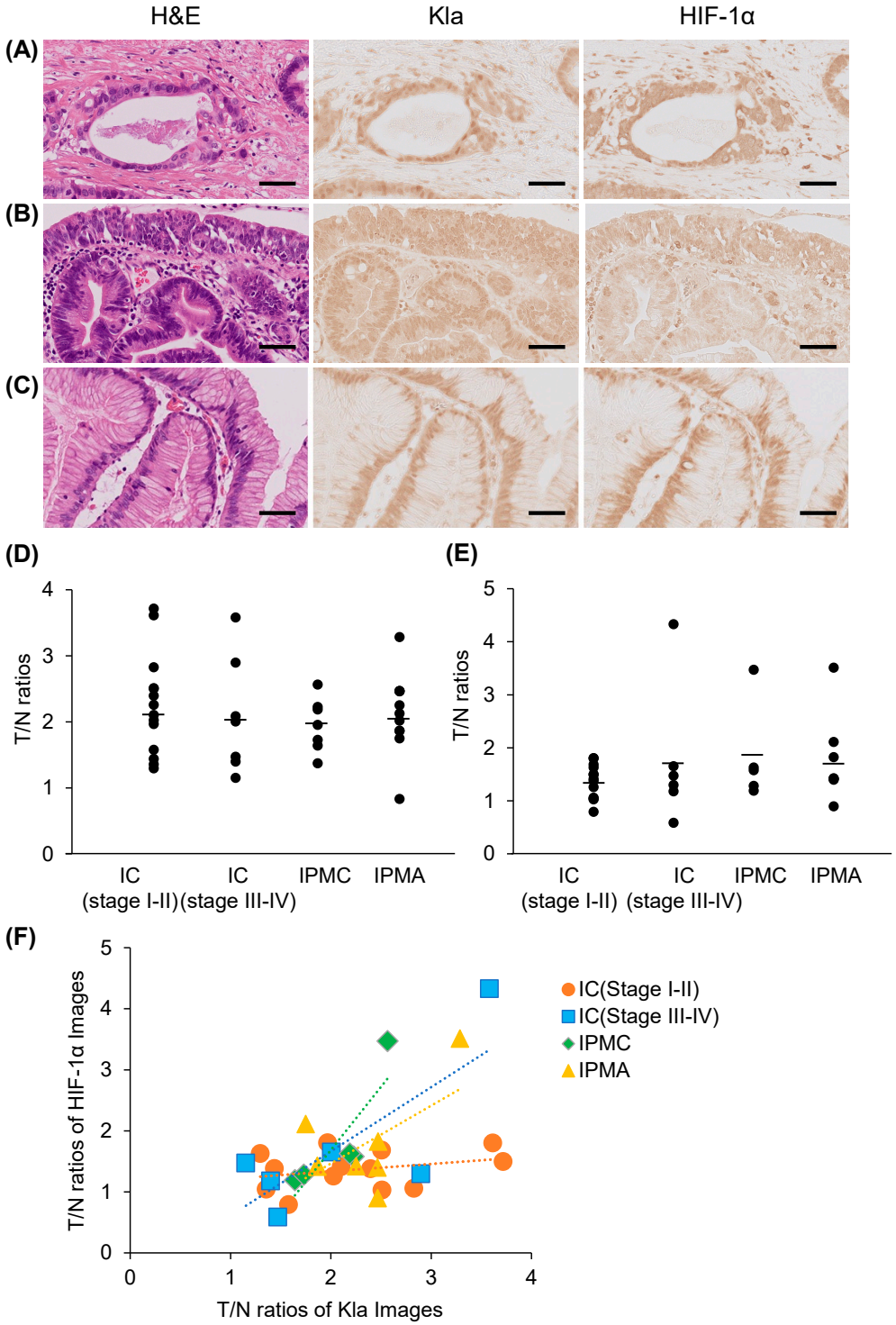

Fig. 2. Immunohistochemical analysis of protein lactylation in human pancreatic tumors. Representative images of invasive carcinoma (IC), non-invasive intraductal papillary mucinous carcinoma (IPMC), and intraductal papillary mucinous adenoma (IPMA) are shown in **A**, **B**, and **C**, respectively. Images of hematoxylin and eosin-stained sections (left panels in **A**, **B** and **C**) as well as of lactyllysine (Kla) (middle panels in **A**, **B** and **C**) and hypoxia-inducible factor 1α (HIF-1α) (right panels in **A**, **B** and **C**) immunohistochemistry (IHC) sections are depicted, respectively. Bars = 50 μm. Ratios between signal intensities in tumor epithelial nuclei and non-tumor duct cell nuclei (T/N ratios) in Kla (**D**) and HIF-1α IHC images (**E**) of invasive carcinoma (IC) (stage I-II) (13 cases, 50 cells per case), IC (stage III-IV) (six cases, 50 cells per case), non-invasive intraductal papillary mucinous carcinoma (IPMC) (six cases, 50 cells per case for Kla analysis) (five cases, 50 cells per case for HIF-1α analysis), and intraductal papillary mucinous adenoma (IPMA) (10 cases, 50 cells per case for Kla analysis) (eight cases, 50 cells per case for HIF-1α analysis). The short horizontal lines show average values. **F**) Relationship between Kla and HIF-1α expression. The relationship of T/N ratios in Kla and HIF-1α IHC images was quantified.

Table 1. *Pathological features of enrolled patients with pancreatic epithelial tumors*

		Age (years)	Sex	Tumor location	Tumor size (mm)	TNM	Stage
Case 1	IC (Stage I-II)	42	M	head	28 × 27 × 28	T2N1M0	IIB
Case 2		64	F	body	30 × 23 × 18	T2N1M0	IIB
Case 3		73	M	body	17 × 11 × 9	T3N0M0	IIA
Case 4		53	M	head	35 × 23 × 21	T3N1M0	IIB
Case 5		74	M	head	17 × 17 × 12	T3N0M0	IIA
Case 6		69	M	head	32 × 29 × 53	T3N1M0	IIB
Case 7		66	M	head	32 × 27 × 21	T2N1M0	IIB
Case 8		64	M	body	16 × 13 × 11	T3N0M0	IIA
Case 9		63	M	head	29 × 25 × 24	T2N1M0	IIB
Case 10		61	M	tail	32 × 23 × 29	T2N1M0	IIB
Case 11		65	F	body	15 × 11 × 43	T3N0M0	IIA
Case 12		47	M	head	7 × 7 × 7	T1cN0M0	I
Case 13		73	F	head	29 × 27 × 27	T2N0M0	IB
Case 14	IC (Stage III-IV)	71	F	body	22 × 18 × 23	T2N0M1	IV
Case 15		70	M	body-tail	90 × 29 × 22	T4N1M0	III
Case 16		66	M	head	80 × 60 × 45	T4N2M0	III
Case 17		73	M	body	75 × 32 × 22	T3N2M0	III
Case 18		72	F	body	16 × 15 × 14	T4N0M0	III
Case 19		81	M	tail	55 × 41 × 64	T4N1M0	III
Case 20	IPMC (non-invasive)	59	F	head	N/A	TisN0M0	0
Case 21		61	M	head	N/A	TisN0M0	0
Case 22		42	M	body	N/A	TisN0M0	0
Case 23		74	M	body	N/A	TisN0M0	0
Case 24		66	M	head	N/A	TisN0M0	0
Case 25		69	F	head	N/A	TisN0M0	0
Case 26	IPMA	61	M	MD	N/A	N/A	N/A
Case 27		53	M	BD	N/A	N/A	N/A
Case 28		69	M	BD	N/A	N/A	N/A
Case 29		61	M	BD	N/A	N/A	N/A
Case 30		61	F	BD	N/A	N/A	N/A
Case 31		64	M	BD	N/A	N/A	N/A
Case 32		63	F	MD	N/A	N/A	N/A
Case 33		50	M	BD	N/A	N/A	N/A
Case 34		61	M	Mix	N/A	N/A	N/A
Case 35		61	M	Mix	N/A	N/A	N/A
Case 36	MCA	44	F	body	N/A	N/A	N/A
Case 37	SCA	56	F	body	N/A	N/A	N/A
Case 38		35	F	N/A	N/A	N/A	N/A

IC, invasive carcinoma; IPMC, intraductal papillary mucinous carcinoma; IPMA, intraductal papillary mucinous adenoma; MCA, mucinous cystadenoma; SCA, serous cystadenoma; M, male; F, female; MD, main duct; BD, branch duct; N/A, not available.

Statistical analysis

Statistical significance was evaluated using Welch's or the Student's t-test in Prism 9 (ver. 9.2.0) (GraphPad Software, Inc., Boston, Massachusetts, USA) or using one way analysis of variance (one-way ANOVA) in Excel 2019 MSO 64 bit (Microsoft Corporation, Redmond, Washington, USA). A p value of <0.05 was considered significant.

III. Results

Clinical study

Thirty-eight patients with pancreatic epithelial tumors who underwent surgery were included in the analysis (Table 1). The study population consisted of 26 men and 12 women, aged between 42 and 81 and 35–73 years, respectively.

Lysine lactylation in human pancreatic non-tumor tissues

A representative image of H&E-stained non-tumor pancreatic epithelial tissue (Fig. 1A) and an image of Kla IHC (low-magnification view: Fig. 1B; medium-magnification view: Fig. 1C) are shown. The arrowheads and arrows in Fig. 1C indicate interlobular duct and acinar cells. IHC images revealed weak positive signals for Kla in both interlobular duct cells and acinar cells. The ratios between SI in the nuclei and cytoplasm in ten Kla IHC images ranged from 1.07 to 2.00 (mean and standard error: 1.40 ± 0.10) for duct cells and 1.17 to 1.78 (1.44 ± 0.06) for acinar cells, indicating greater lysine lactylation in nuclei than in the cytoplasm (Fig. 1D).

Lysine lactylation is upregulated in pancreatic epithelial tumor tissues

The thirty-eight resected tumor tissues were classified

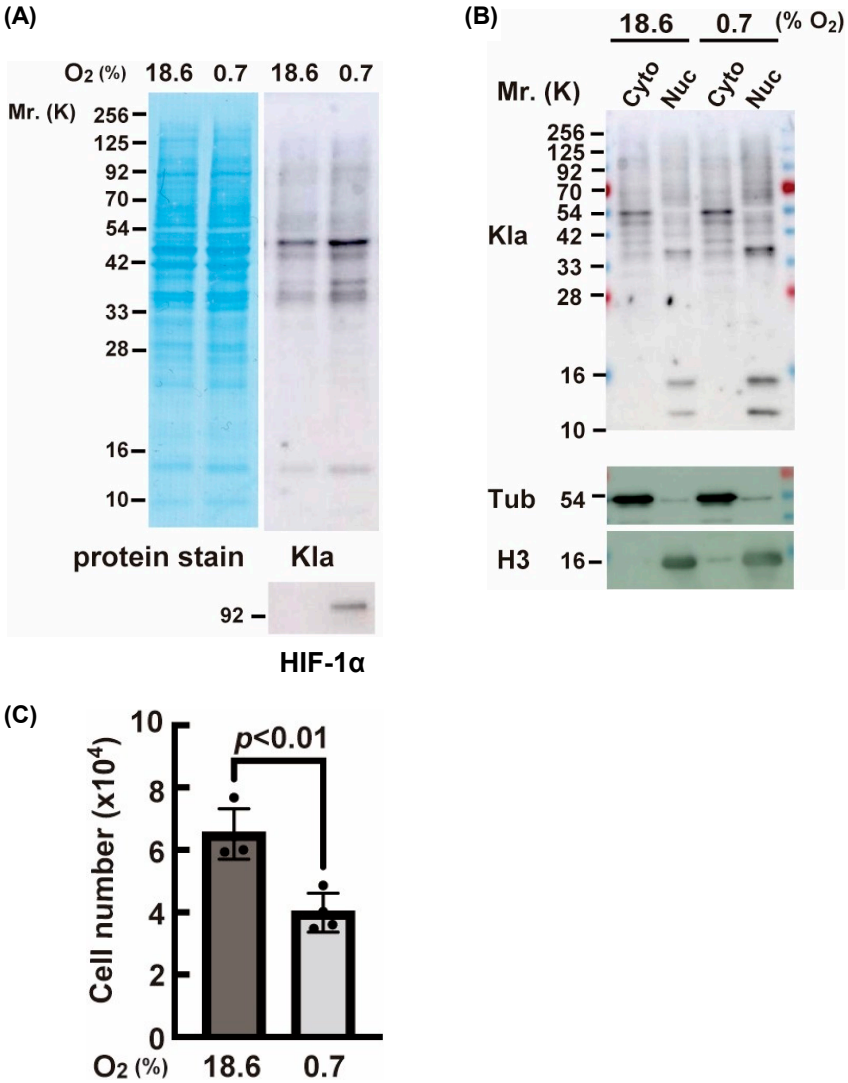

Fig. 3. Hypoxia-induced protein lactylation of cellular proteins *in vitro*. PANC-1 cells were allowed to grow under normoxic (18.6% O_2) or severe hypoxic (0.7% O_2) conditions for 48 hr. Whole-cell lysates were then immunoblotted with an antibody against lactyllysine or HIF-1α (**A**). Alternatively, whole cell lysate was fractionated into nuclear (Nuc) and cytoplasmic (post-nuclear supernatant) factions (Cyto), followed by immunoblotting with antibody against lactyllysine (**B**). Successful fractionation was confirmed by re-probing with antibody against β-tubulin (Tub) (cytoplasmic marker) or histone H3 (nuclear marker). The number of living cells was shown in (**C**). Kla, lactyllysine. HIF-1α, hypoxia-inducible factor 1α.

into 19 cases of invasive carcinoma (IC), including invasive ductal carcinoma and invasive intraductal papillary mucinous carcinoma (IPMC); six cases of non-invasive IPMC; 10 cases of IPMA; one case of mucinous cystadenoma (MCA); and two cases of serous cystadenoma (SCA) (Table 1). Tissue samples from IC, noninvasive IPMC, and IPMA were evaluated, with representative images shown in Fig. 2A, 2B and 2C, respectively (left panels; H&E staining, middle panels; Kla IHC, right panels; HIF-1α IHC). Strong Kla signals were noted in the nuclei of all three neoplasm types, with signals stronger than those in the cytoplasm (middle panels of Fig. 2A, 2B and 2C). HIF-1α signals were also observed mainly in the nuclei of neoplastic cells (right panels of Fig. 2A, 2B and 2C). The Kla SI ratio between tumor and duct cell nuclei ranged from 1.30 to 3.72 (2.26 ± 0.22) for IC (stage I-II), 1.15 to 3.58 (2.08 ± 0.39) for IC (stage III–IV), 1.37 to 2.56 (1.95 ± 0.18) for non-invasive IPMC, and 0.83 to 3.29 (2.13 ± 0.20) for IPMA, respectively (Fig. 2D). There were no significant differences in the average SI ratios among IC, noninvasive IPMC, and IPMA. Semi-quantitative evaluation of HIF-1α expression revealed elevated SI ratios between tumor and duct cell nuclei [1.37 ± 0.09 for IC (stage I–II), 1.75 ± 0.54 for IC, 1.83 ± 0.42 for non-invasive IPMC, 1.75 ± 0.28 for IPMA] (Fig. 2E). Next, the relationship between Kla and HIF-1α expression in tumors was evaluated. As shown in the scatter plot of the SI ratios of Kla and HIF-1α in Fig. 2F, Kla and HIF-1α expression were correlated [r = 0.301 for IC (stage I–II), r = 0.770 for IC (stage III–IV), r = 0.845 for non-invasive IPMC, and r = 0.597 for IPMA]. Supple-

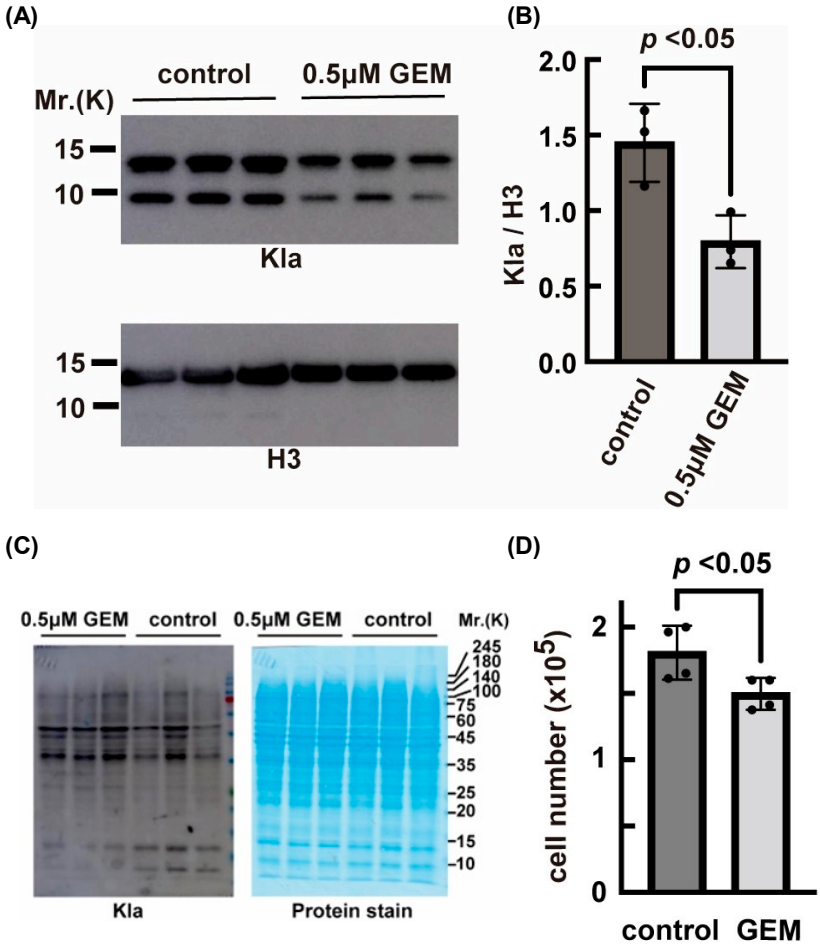

Fig. 4. Effect of gemcitabine (GEM) on histone lactylation. PANC-1 cells were cultured in the absence or presence of 0.5 μM GEM for 36 hr. Histones were extracted from the treated cells and subjected to immunoblotting with antibodies against lactyllysine or histone H3 (**A**). The signal intensity of lactyllysine normalized to that of histone H3 is shown (**B**). Alternatively, whole-cell lysate was also subjected to immunoblotting with an antibody against lactyllysine (**C**, left panel). Proteins on the blot were visualized via CBB R250 staining (**C**, right panel). The number of living cells is shown in (**D**). Kla, lactyllysine.

mentary Figure S1 shows representative H&E and Kla IHC high-magnification images of the MCA and SCA. In both, Kla was observed mainly within nuclei (arrows in Supplementary Fig. S1A and S1B).

Hypoxia induces an increase in global protein lactylation

To assess the effects of hypoxia on protein lactylation, PANC-1 cells were allowed to grow under normoxic or severely hypoxic conditions (0.7% of O_2). As shown in Fig. 3A, hypoxia upregulated global protein lactylation. Hypoxic adaptation was confirmed based on HIF-1α levels (lower panel of Fig. 3A), whose stabilization is known to be increased under hypoxic stress. Consistent with the histopathological observations, subcellular fractionation indicated that some prominent lactylated proteins (approximately 35, 15, and 10 kDa protein) were localized in nuclear fraction. (Fig. 3B), regardless of oxygen tension. Severe hypoxic conditions significantly suppressed cell proliferation down to approximately 60% compared of control levels (Fig. 3C), consistent with previous studies [14, 30].

Effects of GEM and SB on histone lactylation

Owing to a high abundance of basic amino acid residues, histones are preferential targets for a variety of PTMs on lysine residues (e.g., acetylation, methylation, monoubiquitination, and lactylation) [12], which modulate chromatin remodeling associated with gene expression or DNA replication. Further, histone acetylation has been implicated in the anti-cancer effects of GEM [19], a first-line chemotherapy drug for PC. Thus, we sought to explore the possible relationship between histone lactylation and the response to GEM *in vitro*. GEM decreased the lactylation level of core histones by approximately 50% compared to that in untreated cells (Fig. 4A and 4B). Core histones consist of four subunits: H3, H2A, H2B, with apparent

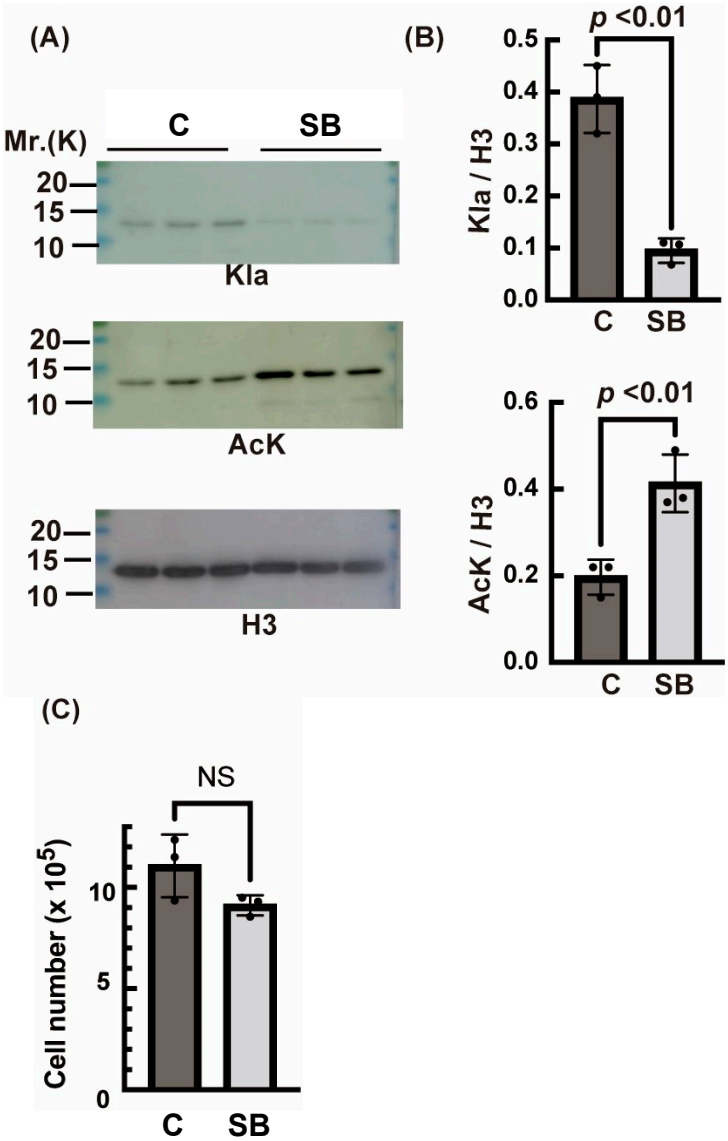

Fig. 5. Effect of sodium butyrate (SB) on histone lactylation. PANC-1 cells were cultured in the presence of 1 mM NaCl (control; C) or 1 mM sodium butyrate (SB) for 35 hr. Histones were purified from the treated cells and subjected to immunoblotting with an antibody to lactyllysine. The blot was subsequently re-probed with antibodies to acetyllysine (AcK) or histone H3 (**A**). The graphs show the signal intensity of lactylated or acetylated proteins normalized to that of histone H3 (**B**). The number of living cells is shown in (**C**). Kla, lactyllysine. C, control. NS, not significant.

molecular weights of approximately 15 kDa, and H4 with apparent molecular weight of approximately 10 kDa on SDS-gel electrophoresis. Judged from their molecular weights in western blotting, the upper and lower signals are considered to be H3/H2A/H2B and H4, respectively (Fig. 4A). Notably, GEM had little effect on global protein lactylation (Fig. 4C), indicating that the GEM-induced decrease in lactylation was limited to specific targets, including histones. GEM suppressed cell growth by approximately 80% compared to controls (Fig. 4D).

Regarding PTMs on lysine residues of histones, a previous study showed that GEM increased histone acetylation [19], which is regulated by histone deacetylates and histone acetyl transferases. Considering our present finding that GEM decreased histone lactylation, change in lactylation could be linked to that in acetylation in histone. To address the possibility, the levels of histone lactylation and acetylation were evaluated after long-term treatment (35 hr) with SB, a broad-spectrum histone deacetylase inhibitor (Fig. 5). SB reduced the lactylation level of core histones by approximately 75%, while increasing their acetylation by 100% (Fig. 5A and 5B). There was no notable difference in viability between SB-treated and control cells (Fig. 5C).

IV. Discussion

While protein lactylation is an established PTM, its pathophysiological significance in tumors remains elusive.

In this study, we showed prominent lysine lactylation in the nuclei of human IC, non-invasive IPMC, and IPMA, which was correlated with HIF-1α expression. *In vitro* experiments using the PC cell line PANC-1 revealed an increased protein lactylation under hypoxic conditions mimicking the tumor microenvironment. Treatment with a low concentration of GEM suppressed histone lactylation as did treatment with histone deacetylase inhibitor SB, suggesting a possible competition between lactylation and acetylation.

Immunohistochemical analysis of protein lactylation in pancreatic tumor tissues showed revealed an increase not only in carcinomas but also in precancerous IPMA. The Warburg effect, characterized by greater lactate production, is observed in proliferating cells, cancer cells included [23]. Further, lactate production is enhanced in precancerous lesions [5]. This may explain the enhanced protein lactylation in noted in precancerous IPMA.

Considering that protein lactylation is associated with energy metabolism under hypoxia, the role of this PTM in tumor formation represents an intriguing matter. Given that a small population of IPMA cells give rise to pancreatic cancer, our findings suggest that lactylation-associated epigenetic changes support cell proliferation and precede the onset of malignant transformation. In this regard, the etiological role of lactylation in pancreatic tumors might be different from that in gastric cancer, where lactylation reportedly increases with malignancy [26]. At present, it is not clear how greater lactylation would promote cell proliferation and the adenoma-adenocarcinoma sequence. Intriguingly, in colorectal adenoma/adenocarcinoma, these processes are promoted through beta-catenin [11], which is activated by hypoxia-induced lactylation [13]. The increased lactylation might affect transformation of benign pancreatic tumor through Wnt/β-catenin signaling pathway [16].

We revealed that histone lactylation status is affected by the anti-cancer drug GEM, whose anti-cancer effect is mediated through the inhibition of DNA synthesis [27]. While we did not define the entire mechanism of GEM-induced histone delactylation, Amrutkar *et al.* recently reported that GEM resistance is induced via glycolysis enhanced by LDHA and MCT4, a transmembrane lactate transporter, in pancreatic cancer cells [2]. Considering that the glycolytic pathway is linked to histone lactylation [10], our findings suggest that histone lactylation could be relevant to therapeutic efficacy of GEM. A previous study suggested that GEM cytotoxicity was synergistically enhanced by SB [15], a broad-specific histone deacetylase inhibitor. While SB increased histone acetylation, it suppressed histone lactylation in the current work (Fig. 5), supporting the above-described hypothesis. However, further studies are required to confirm such synergy.

It should be noted that there are some limitations to our study. First, we could not examine the relationship between prognosis and protein lactylation because the number of cases examined was relatively small. In the future, we would like to increase the number of cases and conduct further analyses. Second, individual lactylated proteins within tumor nuclei have not been characterized in the surgically resected samples. We intend to conduct this by means of proteomics. Finally, we did not conduct experiments on the molecular mechanism underlying the effect of GEM on lactylation, nor did we conduct experiments using GEM-resistant PANC-1 cells. We plan to pursue this experimental direction in the near future.

In conclusion, we provide evidence for the possible involvement of protein lactylation in the development of pancreatic epithelial tumors as well as in the response to GM. Pharmacological targeting of energy metabolism-associated PTMs holds potential for the treatment of PC, which is characterized by a poor prognosis. Although further detailed analyses are required, our findings establish a basis for the involvement of protein lactylation in the pathogenesis of pancreatic epithelial tumors.

V. Conflicts of Interest

The authors declare that they have no conflict of interest.

VI. Funding

This work was partially funded by the Japan Science and Technology Agency/Core Research for Evolutional Science and Technology (grant number: JPMJCR1925), the Japan Society for the Promotion of Science (grant number: 23K06499), and the Research Program of "Network Joint Research Center for Materials and Devices research area" (grant number: 20233002).

VII. Acknowledgments

We thank Mr. Toshifumi Kawamura and Mr. Takashi Okuda of Kyoto Prefectural University of Medicine for their technical assistance.

VIII. References

1. Annual Report to the Nation: Cancer deaths continue downward trend; modest improvements in survival for pancreatic cancer. Available online: https://www.nih.gov/news-events/news-releases/annual-report-nation-cancer-deaths-continue-downward-trend-modest-improvements-survival-pancreatic-cancer (accessed on 18 Jan 2024).
2. Amrutkar, M., Berg, K., Balto, A., Skilbrei, M. G., Finstadsveen, A. V., Aasrum, M., *et al.* (2023) Pancreatic stellate cell-induced gemcitabine resistance in pancreatic cancer is associated with LDHA- and MCT4-mediated enhanced glycolysis. *Cancer Cell Int.* 23; 9.
3. Brierley, J. D., Gospodarowicz, M. K. and Wittekind, C. (2017) TNM Classification of Malignant Tumours, John Wiley & Sons, Hoboken, USA.
4. Cancer Stat Facts: Pancreatic Cancer. Available online: https://seer.cancer.gov/statfacts/html/pancreas.html (accessed on 18 Jan 2024).

5. Chen, X., Yi, C., Yang, M. J., Sun, X., Liu, X., Ma, H., *et al.* (2021) Metabolomics study reveals the potential evidence of metabolic reprogramming towards the Warburg effect in precancerous lesions. *J. Cancer* 12; 1563–1574.
6. Domagała-Haduch, M., Robek, A., Wnuk, J., Michalecki, Ł. and Gisterek, I. (2023) Analysis of the efficacy and tolerability of FOLFIRINOX chemotherapy treatment in patients over 65 years of age with diagnosis of advanced adenocarcinoma of the pancreas. *Contemp. Oncol. (Pozn.)* 27; 10–13.
7. Galle, E., Wong, C. W., Ghosh, A., Desgeorges, T., Melrose, K., Hinte, L. C., *et al.* (2022) H3K18 lactylation marks tissue-specific active enhancers. *Genome Biol.* 23; 207.
8. Li, X., Jiang, Y., Meisenhelder, J., Yang, W., Hawke, D. H., Zheng, Y., *et al.* (2016) Mitochondria-Translocated PGK1 Functions as a Protein Kinase to Coordinate Glycolysis and the TCA Cycle in Tumorigenesis. *Mol. Cell* 61; 705–719.
9. Lin, J., Liu, G., Chen, L., Kwok, H. F. and Lin, Y. (2022) Targeting lactate-related cell cycle activities for cancer therapy. *Semin. Cancer Biol.* 86; 1231–1243.
10. Merkuri, F., Rothstein, M. and Simoes-Costa, M. (2024) Histone lactylation couples cellular metabolism with developmental gene regulatory networks. *Nat. Commun.* 15; 90.
11. Miao, Z., Zhao, X. and Liu, X. (2023) Hypoxia induced β-catenin lactylation promotes the cell proliferation and stemness of colorectal cancer through the wnt signaling pathway. *Exp. Cell Res.* 422; 113439.
12. Millán-Zambrano, G., Burton, A., Bannister, A. J. and Schneider, R. (2022) Histone post-translational modifications - cause and consequence of genome function. *Nat. Rev. Genet.* 23; 563–580.
13. Murakami, T., Mitomi, H., Saito, T., Takahashi, M., Sakamoto, N., Fukui, N., *et al.* (2015) Distinct WNT/β-catenin signaling activation in the serrated neoplasia pathway and the adenoma-carcinoma sequence of the colorectum. *Mod. Pathol.* 28; 146–158.
14. Nisar, H., Sanchidrián González, P. M., Brauny, M., Labonté, F. M., Schmitz, C., Roggan, M. D., *et al.* (2023) Hypoxia Changes Energy Metabolism and Growth Rate in Non-Small Cell Lung Cancer Cells. *Cancers (Basel)* 15; 2472.
15. Panebianco, C., Villani, A., Pisati, F., Orsenigo, F., Ulaszewska, M., Latiano, T. P., *et al.* (2022) Butyrate, a postbiotic of intestinal bacteria, affects pancreatic cancer and gemcitabine response in in vitro and in vivo models. *Biomed. Pharmacother.* 151; 113163.
16. Ram Makena, M., Gatla, H., Verlekar, D., Sukhavasi, S., Pandey, M. K. and Pramanik, K. C. (2019) Wnt/β-Catenin Signaling: The Culprit in Pancreatic Carcinogenesis and Therapeutic Resistance. *Int. J. Mol. Sci.* 20; 4242.
17. Sarvepalli, D., Rashid, M. U., Rahman, A. U., Ullah, W., Hussain, I., Hasan, B., *et al.* (2019) Gemcitabine: A Review of Chemoresistance in Pancreatic Cancer. *Crit. Rev. Oncog.* 24; 199–212.
18. Sharma, R., Nakamura, A., Takahashi, R., Nakamoto, H. and Goto, S. (2006) Carbonyl modification in rat liver histones: decrease with age and increase by dietary restriction. *Free Radic. Biol. Med.* 40; 1179–1184.
19. Shimizu, K., Nishiyama, T. and Hori, Y. (2017) Gemcitabine Enhances Kras-MEK-Induced Matrix Metalloproteinase-10 Expression Via Histone Acetylation in Gemcitabine-Resistant Pancreatic Tumor-initiating Cells. *Pancreas* 46; 268–275.
20. Słodkowski, M., Wroński, M., Karkocha, D., Kraj, L., Śmigielska, K. and Jachnis, A. (2023) Current Approaches for the Curative-Intent Surgical Treatment of Pancreatic Ductal Adenocarcinoma. *Cancers (Basel)* 15; 2584.
21. Sørensen, B. S. and Horsman, M. R. (2020) Tumor Hypoxia: Impact on Radiation Therapy and Molecular Pathways. *Front. Oncol.* 10; 562.
22. Uzunparmak, B. and Sahin, I. H. (2019) Pancreatic cancer microenvironment: a current dilemma. *Clin Transl Med.* 8; 2.
23. Vander Heiden, M. G., Cantley, L. C. and Thompson, C. B. (2009) Understanding the Warburg effect: the metabolic requirements of cell proliferation. *Science* 324; 1029–1033.
24. Vaupel, P. and Multhoff, G. (2021) Revisiting the Warburg effect: historical dogma versus current understanding. *J. Physiol.* 599; 1745–1757.
25. Wang, N., Wang, W., Wang, X., Mang, G., Chen, J., Yan, X., *et al.* (2022) Histone Lactylation Boosts Reparative Gene Activation Post-Myocardial Infarction. *Circ. Res.* 131; 893–908.
26. Yang, D., Yin, J., Shan, L., Yi, X., Zhang, W. and Ding, Y. (2022) Identification of lysine-lactylated substrates in gastric cancer cells. *iScience* 25; 104630.
27. Yang, S., Luo, D., Li, N., Li, C., Tang, S. and Huang, Z. (2020) New Mechanism of Gemcitabine and Its Phosphates: DNA Polymerization Disruption via 3'-5' Exonuclease Inhibition. *Biochemistry* 59; 4344–4352.
28. Ying, H., Kimmelman, A. C., Lyssiotis, C. A., Hua, S., Chu, G. C., Fletcher-Sananikone, E., *et al.* (2012) Oncogenic Kras maintains pancreatic tumors through regulation of anabolic glucose metabolism. *Cell* 149; 656–670.
29. Zhang, D., Tang, Z., Huang, H., Zhou, G., Cui, C., Weng, Y., *et al.* (2019) Metabolic regulation of gene expression by histone lactylation. *Nature* 574; 575–580.
30. Zhao, H., Chen, W., Zhu, Y. and Lou, J. (2021) Hypoxia promotes pancreatic cancer cell migration, invasion, and epithelial-mesenchymal transition via modulating the FOXO3a/DUSP6/ERK axis. *J. Gastrointest. Oncol.* 12; 1691–1703.
31. Zhong, H., De Marzo, A. M., Laughner, E., Lim, M., Hilton, D. A., Zagzag, D., *et al.* (1999) Overexpression of hypoxia-inducible factor 1alpha in common human cancers and their metastases. *Cancer Res.* 59; 5830–5835.